

Determination of radiative lifetimes of neutral sulphur by time-resolved three-photon VUV laser spectroscopy

Z.S. Li¹, A. Persson¹, S. Svanberg^{1,a}, H.P. Garnir², and E. Biémont²

¹ Department of Physics, Lund Institute of Technology, P.O. Box 118, 221 00 Lund, Sweden

² Institut d'Astrophysique, Université de Liège, 5 avenue de Cointe, 4000 Liège, Belgium

Received: 9 February 1998 / Accepted: 24 February 1998

Abstract. Radiative lifetimes of the highly excited states $3p^3 8s\ ^3S_1^0$ and $3p^3 6d\ ^3D_{1,2,3}^0$ of neutral sulphur have been measured using time-resolved laser-induced fluorescence. The sulphur atoms were generated in a laser-produced plasma. The investigated states were populated through a two-step process involving a two-photon excitation to the lowest excited triplet state of even parity $3p^4\ ^3P_{0,1,2}$, followed by a one-photon excitation to the investigated state. We obtained $\tau(8s\ ^3S_1^0) = 40 \pm 5$ ns and $\tau(6d\ ^3D_{1,2,3}^0) = 75 \pm 7$ ns. These values are much longer than theoretically predicted ones and much shorter than those indirectly inferred from astronomical data.

PACS. 32.70.Ca Oscillator and band strengths, lifetimes, transition moments, and Franck-Condon factors
– 42.62.Fi Laser spectroscopy

1 Introduction

A large number of sulphur atomic lines have been observed in the solar photospheric spectrum as well as in other astronomical objects [1, 2]. In view of the high cosmic abundance values, astrophysicists are interested in accurate spectroscopic data of this element [3]. However, only a small number of the experimental oscillator strengths needed are available from literature [4], since considerable practical difficulties exist. Firstly, an ordinary electrically-heated oven can only evaporate sulphur molecules. Secondly, most of the resonance transitions from the ground state are in the VUV region. Part of the S I energy level diagram is shown in Figure 1. The ground-state configuration of the sulphur atom is $3p^4$, where one of the $3p$ electrons can be excited forming $3p^3 nl$ states. From the ground-state levels, most of the excited states are reachable only in the VUV region if single-photon transitions are used. This results in great difficulties both for the excitation and for the following fluorescence detection. Recently, two laser spectroscopic investigations have been performed at the Lund Laser Centre (LLC) on radiative lifetimes of excited states of atomic sulphur. Zerneck *et al.* [5] measured the lifetimes of the $4p\ ^3P_{0,1,2}$ and $5p\ ^3P_{1,2}$ states. Time resolved two-photon laser spectroscopy was used. The $4p$ and $5p$ states were populated using two UV photons from the ground-state levels, and subsequently cascade fluorescence light was observed. Berzinsh *et al.* [6] measured the radiative lifetimes of some highly excited odd-parity states of S I. VUV laser excitation was used

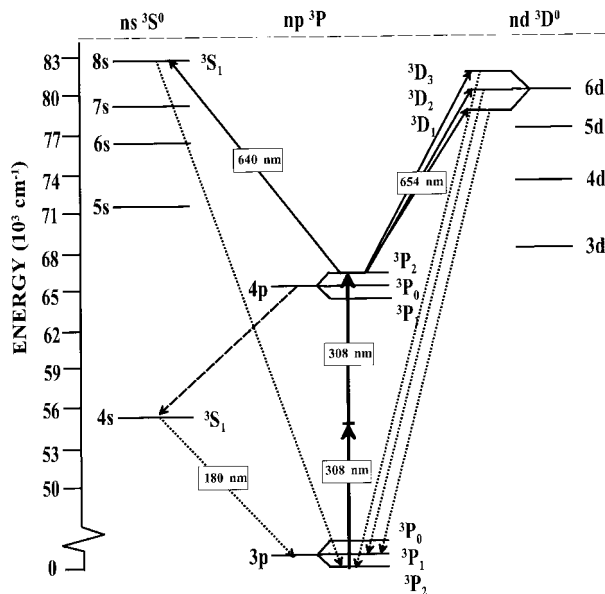


Fig. 1. Partial energy diagram of neutral sulphur (the solid lines indicate the three-photon excitation pathways, while the dashed lines indicate the observed fluorescence).

in order to populate the studied high-lying states directly from the ground-state levels. Accurate lifetime values were evaluated from the recorded fluorescence in both studies.

In the present paper, we report new experimental results of radiative lifetimes of highly excited states of S I. This is a continuation of our previous work.

^a e-mail: sune.svanberg@fysik.lth.se

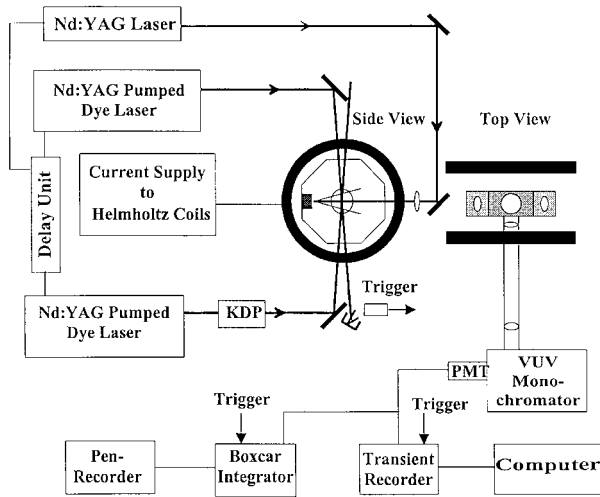


Fig. 2. Experimental set-up for time-resolved laser spectroscopy.

A three-photon excitation scheme has been used to populate the high-lying odd-parity states from the even-parity ground state. The same scheme was successfully used in O I [7] and N I [8]. As indicated in Figure 1, intense 308 nm UV laser light was used as the first step to populate the even-parity $4p\ ^3P_2$ state from the ground state by a two-photon transition. Then, in a second step, a one-photon transition follows, exciting the atom to the $3p^38s\ ^3S_1^0$ or $3p^36d\ ^3D_{1,2,3}^0$ states. VUV fluorescence in the transition directly to the ground state was detected. Lifetimes were evaluated by a fitting of the fluorescence curves to exponential functions.

2 Experimental set-up

The experimental set up is illustrated in Figure 2. Two dye lasers (Continuum ND-60) were pumped by two Nd:YAG lasers (Continuum NY-82). One dye laser, operating on DCM dye, was tuned to 616 nm. The second harmonic, at 308 nm, with a pulse energy of about 25 mJ, was produced in a KDP crystal, and this UV beam was used to populate the $4p$ state through two-photon transitions. Another dye laser, also operating on DCM, was used in a second step to populate the selected high-lying odd-parity states. The two laser beams were sent from opposite directions and were made to cross in the centre of the vacuum chamber. Fluorescence light was collected perpendicularly to the laser beams through two MgF_2 lenses and focused to the slit of a vacuum monochromator (Acton model VM 502) and finally detected by a photomultiplier tube (Hamamatsu R1220). The data acquisition and evaluation were performed by using a digital oscilloscope (Tektronic model DSA 602) and a personal computer. The signal from the photomultiplier tube could also be connected to a BOXCAR averager followed by a pen recorder.

A laser-produced plasma was used as a sulphur atomic source. Pulses of second-harmonic radiation from a Nd:YAG laser (Continuum Surelite) were focused into lead

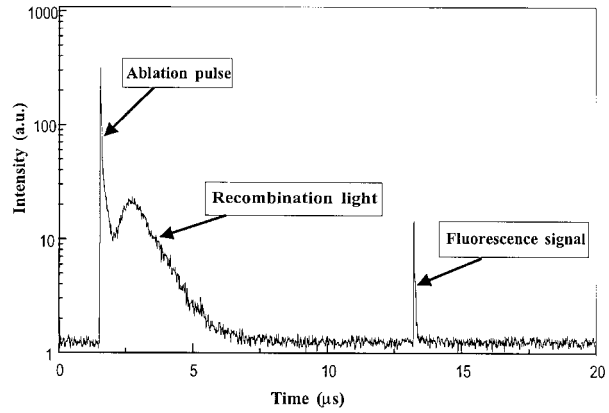


Fig. 3. Detected light intensity around 180 nm as a function of time after the ablation pulse. The signal at about $13\ \mu s$ is laser-induced cascade fluorescence from the $4s\ ^3S_1^0$ state. The signal before $10\ \mu s$ is recombination light from the ions and atoms.

sulphide powder. The powder was confined in a metallic container. A pulse energy of 10-30 mJ caused ablation of the powder, which was splashing at the laser pulse impact. To maintain a smooth target surface for the next laser pulse, the container was shaken by an electromagnet at a frequency in resonance with mechanical vibrations of the magnet/container arrangement.

All three Nd:YAG lasers were externally triggered from a common unit (Stanford Research System model 35). This not only ensured the temporal overlap of the two dye laser pulses but also allowed us to tune time delays between the ablation beam and the excitation beam.

3 Measurement and results

The target was formed by a laser-produced plasma containing sulphur atoms. Just after the ablation pulse, the plasma glows because of the recombination light of ions and atoms. After a few μs , that parasitic light disappears and a sample of atoms is obtained. The curve in Figure 3 was observed by tuning the monochromator to 180 nm; the fluorescence signal as indicated is the cascade transition from $4s$ to $3p$, which was produced by the 308 nm laser two-photon transition (see Fig. 2). It can be seen that after $8\ \mu s$ delay from the ablation beam, there is no plasma background.

The first-step excitation with a two-photon transition was studied by applying the 308 nm beam about $10\ \mu s$ after the ablation pulse. The cascade line of 180 nm fluorescence light was recorded using a BOXCAR integrator and a pen recorder while scanning the dye laser wavelength from 307 nm to 311 nm. Seven lines were observed as illustrated in Figure 4, in agreement with the two-photon transition selection rules given by Bonin and McIlrath [9]. From Figure 4, we selected the transition $^3P_2 \rightarrow ^3P_2$ as the first step and fixed the dye laser wavelength at 308.200 nm. Then the vacuum monochromator was tuned to the 125 nm region and the resolution was set to 2 nm

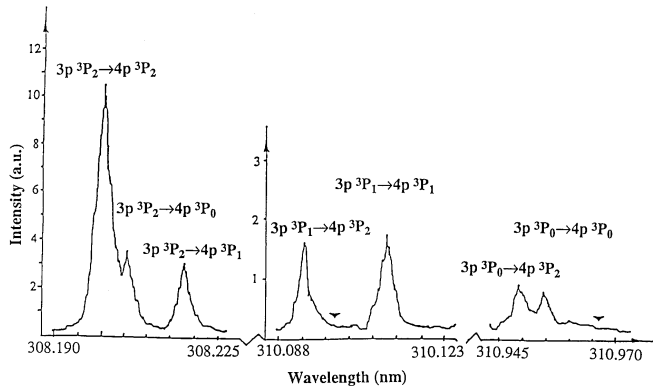


Fig. 4. Detected light intensity around 180 nm as a function of laser wavelength (scanning from 308.190 nm to 311.00 nm) of the first-step two-photon transition. The seven peaks corresponded to transitions $3p\ ^3P_2 \rightarrow 4p\ ^3P_2$ (308.200 nm), $3p\ ^3P_2 \rightarrow 4p\ ^3P_0$ (308.206 nm), $3p\ ^3P_2 \rightarrow 4p\ ^3P_1$ (308.218 nm), $3p\ ^3P_1 \rightarrow 4p\ ^3P_2$ (310.093 nm), $3p\ ^3P_1 \rightarrow 4p\ ^3P_1$ (310.111 nm), $3p\ ^3P_0 \rightarrow 4p\ ^3P_2$ (310.949 nm), $3p\ ^3P_0 \rightarrow 4p\ ^3P_0$ (310.955 nm). Different vertical scales have been used in the different parts of the recording.

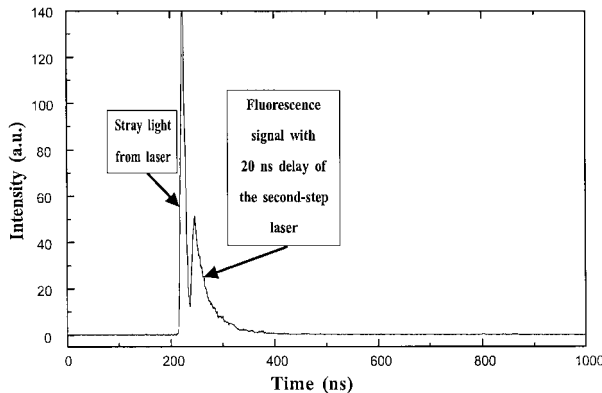


Fig. 5. Time-resolved fluorescence signal recorded at 124.2 nm. Laser stray light and fluorescence due to the $8s\ ^3S_1^0$ state are observed.

(0.5 mm slit). VUV fluorescence to the ground state from the high-lying odd-parity states selectively populated by a following red beam was detected. A typical curve for the $8s\ ^3S_1^0$ state is shown in Figure 5, in which the red beam for the second step has about 20 ns delay from the 308 nm pulse used for the first step (the lifetime of $4p\ ^3P_2$ is 46.1 ns [5]). The delay time could be changed in a controlled way to optimise the fluorescence signal.

Time-resolved laser spectroscopy was used to obtain reliable radiative lifetime values under appropriate experimental conditions. A Helmholtz coil system provided a sufficiently high magnetic field to wash out quantum beats. To eliminate the flight-out-of-view effect, the slit of the detection monochromator was set to be parallel to the flight direction. Effects from collisions between the excited atoms and the residual gas (air) in the chamber were investigated by increasing the background pressure by an order of magnitude. Lifetimes measured under these

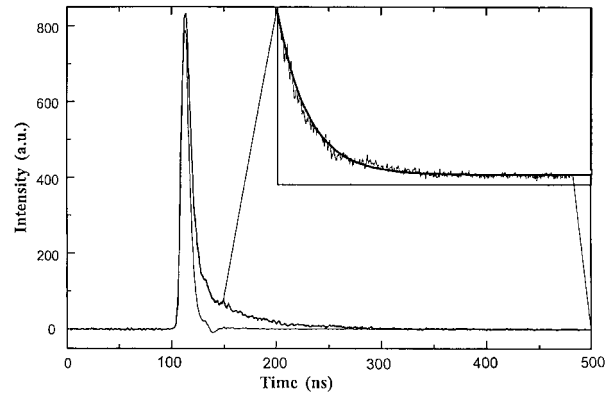


Fig. 6. Typical fluorescence decay curve of the $8s\ ^3S_1^0$ state used for lifetime evaluation. The thick line represents the total signal, the thin line the stray light detected by detuning the monochromator. An exponential fitting is also shown in the upper right corner.

circumstances were not found to be shorter than those obtained at the best achievable background pressure. To make sure that the lifetimes are not affected by radiation trapping and collisions in the laser-produced plasma, experiments were performed with different time delays between the atomisation laser pulse and the excitation lasers. A typical fluorescence decay curve of the state $8s\ ^3S_1^0$ for the final evaluation is shown in Figure 6. The high peak of the front part of the curve was from the stray light of the strong laser pulse (see also Fig. 5). This stray light was due to reflexes in the housing of the monochromator; unfortunately we could not eliminate it. To cancel the effect of this stray light, a stray light curve was recorded by switching off the second-step excitation light beam (the red beam for second-step excitation caused no stray light since the PMT used here is solar-blinded) while keeping all the other conditions constant. In this way the fluorescence signal was completely removed and the stray light component (thin line in Fig. 6) could be recorded and subsequently subtracted from the fluorescent signal (thick line in Fig. 6). A pure fluorescent signal curve was obtained. Such curves were evaluated by making a least-squares fit of an exponential to the recorded time-resolved fluorescence intensity. Only the part of the curve that was recorded after the turn off of the laser pulse was used in the fit. The starting point of this fit was varied to make sure that no deviations from the exponential signal shape influenced the measurement. We found that this evaluation gave the same lifetime value for the curves before and after the subtraction of the stray light.

Only a few photons were detected for each shot to ensure a linear response of the detection system also considering the stray light spike. 4000 shots were accumulated for each record to make a smooth curve. For each state, about 30–40 curves were recorded depending on the conditions. A plot of evaluated lifetimes *versus* delay time for the $8s\ ^3S_1^0$ state is given in Figure 7. The lifetime values evaluated from the curve recorded after a sufficiently long delay from the ablation pulse are used to make an average

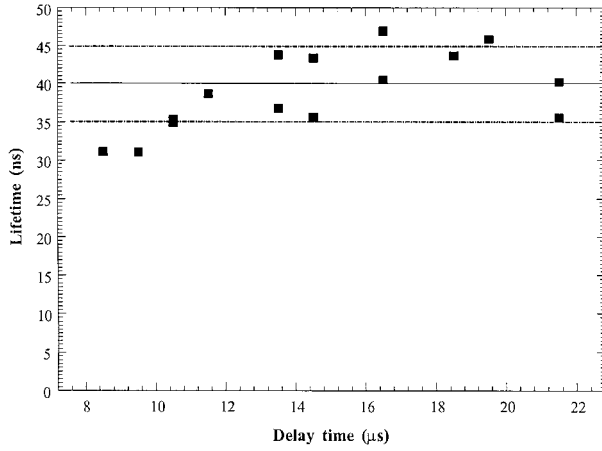


Fig. 7. Measured radiative lifetime of the $8s\ ^3S_1^0$ state as a function of delay time.

Table 1. Measured lifetimes of this work and comparison with other works.

Levels	Energy (cm^{-1})	Lifetime (ns)			
		$\tau_{\text{exp}}^{\text{a}}$	$\tau_{\text{HFR}}^{\text{b}}$	FC ^c	OP ^d
$6d\ ^3D_1$	80185.78	75(7)	16.0	199(90)	227
$6d\ ^3D_2$	80183.93		15.9		
$6d\ ^3D_3$	80182.54		15.8		
$8s\ ^3S_1$	80521.99	40(5)	33.1	73.3	56.2

^a This work: Time-resolved laser spectroscopy.

^b This work: HRF calculations; for details see reference [10].

^c Astronomical sources, reference [3].

^d Calculation performed in the framework of the OPACITY project, reference [11].

for the final lifetime value of each state. Two standard deviations are taken as the error bars. Final results are listed in Table 1.

The three sublevels of $6d\ ^3D_{1,2,3}^0$ have been measured separately. Since the difference in these lifetime values is

very small, we give the same lifetime value for all three sublevels.

We found, that the lifetime values of the $6d$ states are longer than that for the $8s$ state, which is in agreement with the trend of the astrophysical data observed by Federman and Cardelli [3]. Large deviations exist when comparing the new results with the theoretical values by Biémont *et al.* [10], which calls for more accurate theoretical calculations.

The authors are grateful to U. Berzinsh for valuable discussions. This work has been partly supported by the European Community Access to Large-Scale Facilities Programme (Contract ERBFMGECT 950020). Financial support from the Swedish National Science Research Council (NFR) and the Belgium National Fund for Scientific Research (FNRS) is also gratefully acknowledged.

References

1. D.L. Lambert, B. Warner, *Mont. Not. R. Astron. Soc.* **138**, 181 (1968).
2. D.C. Morton, *Ap. J. Supp.* **77**, 119 (1991).
3. S.R. Federman, J.A. Cardelli, *Ap. J.* **452**, 269 (1995).
4. E. Biémont, P. Quinet, C.J. Zeippen, *Astron. Astrophys. Sup.* **102**, 435 (1993).
5. R. Zerne, C.Y. Luo, U. Berzinsh, S. Svanberg, *Phys. Scr.* **56**, 459 (1997).
6. U. Berzinsh, C.Y. Luo, R. Zerne, S. Svanberg, *Phys. Rev. A* **55**, 1836 (1997).
7. S. Kröll, H. Lundberg, A. Persson, S. Svanberg, *Phys. Rev. Lett.* **55**, 284 (1985).
8. G.J. Bengtsson, J. Larsson, S. Svanberg, D.D. Wang, *Phys. Rev. A* **45**, 2712 (1992).
9. K.D. Bonin, T.J. McIlrath, *J. Opt. Soc. Am. B* **1**, 52 (1984).
10. E. Biémont, H.P. Garnir, S.R. Federman, Z.S. Li, S. Svanberg, (1998) *Astrophys. J.* (in press).
11. K. Butler, C. Mendoza, C.J. Zeippen, (1998) (to be published).